Magnetic Spectrographs

Magnetic analysis continues to be an unusually effective technique for nuclear-structure studies. Improved spectrograph designs combine high resolution with the rapid collection of very large amounts of data.

by Harald A. Enge

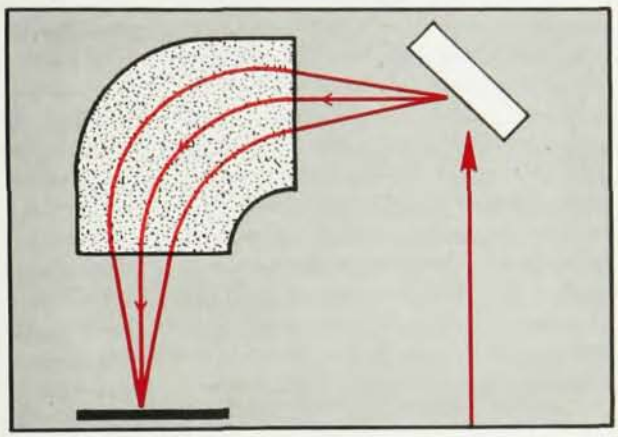

MAGNETS HAVE BEEN USED as experimental aids in nuclear physics since the earliest days of radioactivity studies. From the first crude devices used 60 years ago to the modern charged-particle spectrographs used today, there has been a tremendous increase in complexity and utility of these instruments and, of course, an accompanying increase in weight and cost—sometimes by as much as a factor of 10^5.

Basically a magnetic spectrograph is used for determining momenta of charged particles emitted from radioactive nuclei or in nuclear reactions or scattering processes. If the identity of the particle is also known (that is, its rest mass), then the energy can be calculated. In nuclear-structure physics, where the energies of the particles detected are of the order of MeV's, the magnetic spectrograph has always faced competition from various detectors that can be used for energy determinations: for instance, the ionization chamber, the scintillation counter and the solid-state counter. Competition from the solid-state counter has been the strongest. This is an extremely effective instrument; it is simple and inexpensive, has good inherent resolving power and can be combined with a dE/dx detector so that not only the energy but also the identity of the particle is recorded.

In nuclear-physics research there is an ever-increasing demand for higher resolving power, higher accuracy and better signal-to-background ratio. The solid-state counter has inherent limitations in these areas whereas, practically speaking, no such limitation exists for the magnetic spectrograph. Therefore, in spite of strong competition from the solid-state counter, the magnetic spectrograph has not decreased in popularity. Quite the contrary, an increasing number of nuclear-physics laboratories have acquired or recently ordered such instruments.

In elementary-particle research, the most popular detectors are spark chambers and bubble chambers. Both of these instruments use huge magnets, so that momenta of recorded particles can be studied by direct measurements of track curvatures. This use of the magnetic field is basically the same as in a spectrograph. However, in the usual terminology, a spectrograph is a device that focuses *secondary* particles of identical momentum to a point or a line on a detector and disperses particles of different momenta. Magnets that deflect, focus, and momentum-analyze ion beams from accelerators (*primary* particles) may be identical in design with magnetic spectrographs, but somehow they fail to be recognized as members of this elite class. Rather, they are called "deflecting magnets" or "analyzing magnets" and are part of the beam-handling system or the beam switchyard.

The complexity of events in most high-energy research requires bubble chambers and spark chambers so that

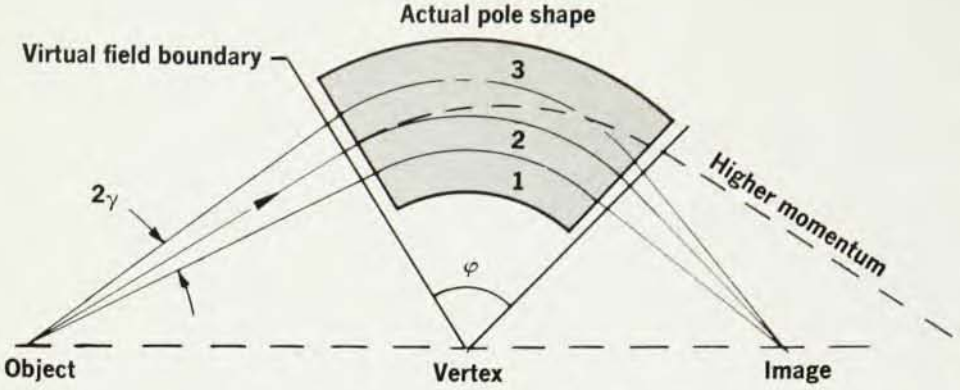

MAGNET sectioned at symmetry (median) plane and showing the shape of the lower pole piece. In the field the orbit is circular. —FIG. 1

the tracks of the reacting particles can be followed in detail. An exception is elastic or inelastic scattering of electrons, which is an important area of research on linear accelerators, notably the Stanford two-mile accelerator. Three huge spectrographs partly for electron-scattering studies were mentioned in a paper by Joseph Ballam in the April issue of PHYSICS TODAY.[1]

Deflection and focusing

In all magnetic spectrographs discussed here the magnetic field is essentially perpendicular to the direction of motion of the particles. The orbits are therefore substantially circular. In some beta spectrographs, which are not discussed here, a large component of the velocity vector is in the direction of the magnetic field. The orbits are then helixes.

For the circular orbit of a particle of mass m, charge q and velocity v, the radius R is given by

$$mv^2/R = qvB \qquad (1)$$

(B is the magnetic induction). We define the *magnetic rigidity* of a particle as the product BR. From equation 1 we obtain

$$BR = mv/q \qquad (2)$$

Born and educated in Norway, Enge has been associated with the MIT Van de Graaff group from 1950–52 and since 1955. He is now professor there. His main interests are nuclear studies and instrumentation.

For particles of the same charge $q = ze$ the orbit radius in a homogeneous field is proportional to the momentum. Equations 1 and 2 are relativistically correct.

In high-energy physics, the convention is to measure the momentum of a particle in MeV/c or GeV/c. For highly relativistic particles, this is numerically equal to the total energy of the particle in MeV or GeV. For low-energy particles this is not a convenient unit. Instead the *mass-energy product* is used and is defined as ME/z^2 with M in atomic mass units (u) and the kinetic energy E in MeV. For nonrelativistic particles, we can write

$$E \approx p^2/2m = (BRq)^2/2m$$

In appropriate units we get

$$BR = 144(ME/z^2)^{1/2} \text{ kilogauss-cm} \qquad (3)$$

Geometric focusing. In principle, the orbit radius for a particle in a magnetic field can be measured by determining three points on the orbit, for instance, by using three slit systems or two slit systems and a photographic plate or other position-sensitive detector. In practice, this is not a desirable method because of the very limited solid angle of acceptance that such an instrument has. Particles emitted in nuclear reactions or scattering processes or from a nuclear decay generally are emitted in all directions. To get a reasonable counting rate, one must construct the instrument to accept particles over a larger solid angle. This design creates a need for focusing action by the instrument. For instruments with two-directional focusing, particles of identical momenta emitted from a point on the source into the acceptance aperture of the instrument ideally will converge after deflection towards a point on the detector. Particles of different momenta will come to a focus at a different point on the detector.

Figure 1 is a section at the symmetry plane (median plane) of a magnet and shows the shape of the lower pole piece. The pole surfaces of this magnet are assumed to be plane and parallel so that inside the pole gap, except close to the boundaries, the field is uniform. The orbit is then a circular arc. In the fringing field close to and outside the edges of the pole pieces, the field decreases rapidly with distance from the magnet, and the radius of curvature of the orbit increases correspondingly. In simple calculations, the fringing field is accounted for, in practice, by assuming that the magnetic field extends with its full value to a *virtual field boundary* (figure 1) and then abruptly drops to zero. The distance from the actual pole-piece boundary to the virtual field boundary is from 0.6 to 0.9 times the air gap, depending upon the size and location of the magnetizing coils.

To find the image point outside the magnet of figure 1 now requires simple geometry. Each of the orbits 1, 2, and 3 consists of a straight line, a circular arc and a straight line, and the reason why 1 and 3 converge toward 2 in the exit space is that the particle following orbit 3 moves a longer distance through the magnetic field and is therefore deflected by a larger angle. Particle 1 moves a shorter distance through the magnetic field and is therefore deflected by a smaller angle. It is not immediately clear, of course, that all three orbits will intersect at one point, and in fact if the virtual field boundaries are straight as indicated, they do not. The resulting aberration of the image increases rapidly with the angle γ. Since a sharp image, that is, clear separation of particles with different momenta, is the objective, the aberration limits the angle of acceptance, which in turn limits the counting rate.

Transverse focusing. In a homogeneous field, there are no transverse forces on the particle to focus in the direction perpendicular to the median plane. However, such forces can be produced in the fringing-field region

of the magnet. Figure 2 shows how a field line curves from the bottom pole piece to the top pole piece. Except in the median plane, the magnetic induction B has a horizontal component. In particular, above the median plane, the magnetic field has a component directed in towards the pole edge. This component is called B_y in the vector diagram of figure 2. If the particle above the median plane passes through the fringing field in a direction different from the normal to the field boundary, it has a y component of velocity, which, combined with the x component of the field produces a z component of the force. In the case shown, this force is directed towards the median plane and is therefore a focusing force. It can easily be shown that, in a first approximation, the focusing impulse that the particle gets in the fringing field is independent of the geometrical shape of the pole corner and the size of the gap. In fact, we find that the fringing field acts on the transverse motion as a lens of focal length

$$f_z = R/\tan\alpha \qquad (4)$$

where R is the orbit radius in the homogeneous field and the *entrance angle* α is illustrated in figure 2. A similar focusing action takes place in the exit fringing field. Equation 4 is reasonably accurate for magnets in which the fringing field drops to a small value in a distance small compared to the radius R. This is the case when the air gap is small compared to the radius; that is, $d/R \ll 1$. The focusing forces in the transverse direction are then strong but of short duration. The theory behind equation 4 is therefore called the *impulse approximation*. In the next higher approximation, one finds

$$R/f_z = \tan\left[\alpha - \frac{Id(1+\sin^2\alpha)}{R\cos\alpha}\right] \qquad (5)$$

I is an integral that varies from 0.4 to 0.7 depending on the shapes of the pole corners and the proximity of the coils.

Median-plane focusing in spectrographs is *vital* because it separates particles of different momenta and produces a sharp momentum spectrum on the recorder. Transverse focusing is *desirable* because it increases the collecting power of the instrument. Also it helps to reduce the spot size on the detector; then a smaller detector can be used with ensuing improvement of signal-to-background ratio.

Inhomogeneous fields. Transverse focusing can also be produced if the field in the median plane tapers off with increasing distance from the center of curvature. In particular, a betatron-type field, which varies with the distance from the center as

$$B = B_0(r_0/r)^{1/2}$$

produces two-directional focusing with the same focusing strength in both planes. In other words, a *sector* magnet with normal entrance and exit and with the field varying according to equation 6 is stigmatic; that is, a point object produces a point image. Because of distortions in the fringing field, this statement does not quite hold in practice unless $d \ll R$. By appropriate choice of entrance and exit angles (α in figure 2), the transverse focusing action in the fringing field of a *homogeneous*-field magnet can be made just as strong as the continuous transverse focusing in the inhomogeneous-field magnet; in fact, the two types of magnets can be made to have almost exactly identical focusing and dispersing properties.

Spectrograph parameters

The usefulness of a spectrograph depends upon such properties as its dispersion, resolution and solid angle of acceptance.

Dispersion. The ability of the magnet to separate particles with different momenta is expressed by the dispersion, defined as

$$D = \frac{\Delta y}{R}\frac{p}{\Delta p} \qquad (7)$$

Here Δp is the change in momentum p that produces a displacement Δy of the central ray (ray 2 in figure 1) as measured at the image.

Resolving power. In the absence of aberration, the resolving power is determined by the size of the source (object). Assume that the object has uniform luminosity and that its width is o, as measured in the median plane perpendicular to the central ray. At the detector, an image is formed with $\Delta y = oM$, where M is the median-plane magnification of the instrument. From equation 7 we find that the resolving power, defined as R.P.$\equiv p/\Delta p$ is given by

$$\text{R.P.} = \frac{D}{M}\frac{R}{o} \qquad (8)$$

Most often, the maximum orbit radius R is determined by the spectrograph designer by considerations of the maximum momentum to be handled and the maximum tolerable field strength B. For maximum resolving power the object size o should, according to equation 8 be as small as possible. For a nuclear-reaction instrument, there is a limit to the intensity that the target can stand; it is also difficult to keep the target-spot position stable. Thus there is a practical lower limit for o of the order of half a millimeter. It is thus clear that to obtain a high resolving power the spectrograph should be designed to have a maximum possible D/M ratio.

Aberrations and solid angle. From the discussion of geometrical focusing above, it is quite obvious that one can design a magnet to bring particles of a given momentum, that is, with a given orbit radius R, to a crossover at exactly the same point even if the opening angle 2γ is very large. One can, for instance, keep the entrance boundary straight and find the appropriate

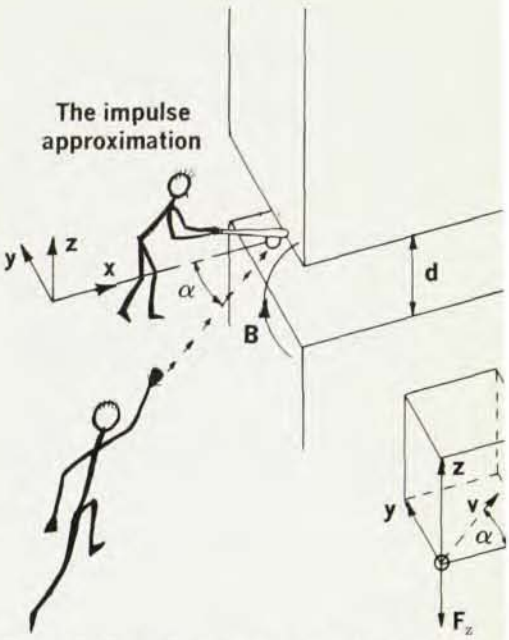

FRINGING-FIELD lines can produce transverse focusing. —FIG. 2

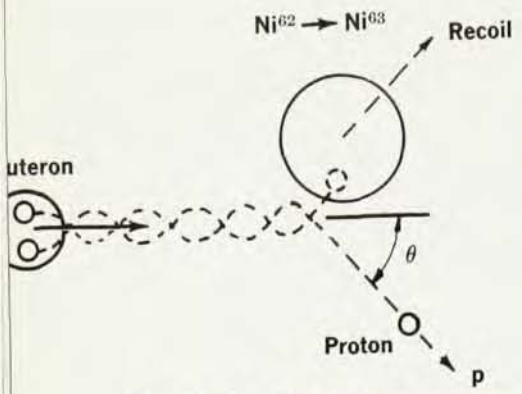

NUCLEAR REACTION emits protons to be analyzed magnetically. —FIG. 3

shape of the exit boundary by a simple geometrical construction. That the field in reality does not drop off abruptly as assumed in the construction is in practice of little consequence.

For particles with higher or lower momenta, however, the focus will in general no longer be perfect; there will be aberrations. Also, if one considers particles moving off the median plane, the situation becomes more complex, and it proves to be impossible to design an instrument with exact point-to-point focusing or even point-to-line focusing unless it has an infinitesimal solid angle of acceptance. For a high-precision spectrograph, the solid angle (that is, the counting rate) is therefore always limited by the aberrations and their effects on the resolving power.

It is customary to express the aberrations as a power series in the entrance half angle γ (figure 1) and the corresponding angle η in the transverse direction. Thus, the aberration in the dispersive plane can be written as

$$\Delta y_{abb} = a_{10}\gamma + a_{20}\gamma^2 + a_{30}\gamma^3 + \cdots + a_{02}\eta^2 + a_{12}\gamma\eta^2 + \cdots \quad (9)$$

Because of symmetry about the median plane, only even-order terms of η appear. The position of the detector can be adjusted so that the first-order term disappears ($a_{10} = 0$). This is what is meant by *first-order* focusing. By appropriate design, the coefficients a_{20} and a_{02} can be made to disappear or to be small at the detector position. The instrument is then *second-order* focusing in the y direction. Most often one need not be concerned about the quality of focus in the transverse direction since this does not affect momentum resolution. For the SLAC electron spectrographs, mentioned earlier in this article, this statement does not hold.

Nuclear-reaction spectrographs

Figure 3 shows as an example the nuclear reaction $Ni^{62}(d,p)Ni^{63}$. A deuteron beam of relatively well defined momentum and direction strikes a target containing Ni^{62} atoms. In the example illustrated, the deuteron breaks up near the surface of the nucleus; the neutron is absorbed by the nucleus; and the proton leaves the collision region at an angle θ with the incident beam. Nuclear-reaction spectroscopy concerns itself with the energy spectrum of the emitted particles and the angular distributions of the energy groups of these particles. The spectrum reflects the energy levels of the residual nucleus Ni^{63}, and the angular distributions and intensities of the various groups yield more specific spectroscopic information about these levels.

There are several features desirable for a magnetic spectrograph used to study particles emitted in nuclear reactions: high resolving power, high intensity (solid angle), high accuracy, high signal-to-background ratio, large angular range (0 to 180 deg ideally), large energy range and provision for Doppler (kinematic) correction. The resolving power has been discussed above with regard to the contribution from the spectrograph itself. The final resolving power achieved in the experiment also depends on the energy homogeneity of the incident beam and the effects of collision with electrons in the target.

The intensity or counting rate, as discussed above, is tied intimately to the resolving power. Presently operating instruments have maximum solid angles of acceptance in the range 0.4 to 10 millisteradians (msr).

The accuracy to which the energy of the emitted particles can be measured is mostly a function of the care with which the spectrograph has been calibrated and ultimately is limited by hysteresis effects in the iron. In a so-called "homogeneous-field" magnet, the field is of course not completely homogeneous but varies typically by about 0.1% from one area of the air gap to another. These variations are caused by inhomogeneities in the air-gap dimensions and are also results of the reluctance of the iron in the pole pieces and yokes. The magnetic properties of iron are such that a given field distribution once measured will never be exactly reproduced. Highest accuracy is, of course, attained with magnets of high-permeability iron.

In nuclear-reaction spectroscopy, the background counts caused by cosmic rays or neutrons hitting the recorder directly are usually very small. The most bothersome background detected takes the shape of a tail on the low-energy side of any intense peak in the spectrum. There are two principal sources for this background: one is lower energy particles in the beam arising partly from scattering off the beam-defining slit edges; the second is scattering from exposed surfaces between the target and the detector. The first source can be minimized by

Nuclear-Reaction Spectrograph Parameters

Type	*Angle φ Degrees*	*Solid angle[a] msr (approx) "normal"*	*max.*	*Momentum range p_{max}/p_{min}*	*D/M (approx)*	*Transverse focusing*	*Focusing corrections[b]*
MIT annular	180	0.4	0.6	1.05	2	No	None
Cal Tech, n = 1/2	180	2.5	6	Small	4	Yes	None
MIT broad-range and multiple gap	90	0.4	1	1.5	2	No	a_{20}[c]
Green's	90	5	10	2.2	3	Approx	$a_{20} \approx 0$
Elbek's	105	1	4	2.5	3	Some	$a_{20} \approx 0$
Split pole	114	2	8	2.7	6	Yes	$a_{20} \approx 0$ a_{02}[c]

[a] In most cases these numbers can be increased by increasing the gap.

[b] Attained resolving power is not quoted because it is a strong function of the solid angle and of extraneous factors. Using full width at half maximum of a peak for Δp, resolving powers exceeding p/Δp = 5000 have been measured.

[c] This coefficient (from equation 9) is zero at one point in the spectrum only.

proper beam cleaning. Transverse focusing in the spectrograph can substantially reduce the second contribution, particularly if the strongest focusing takes place in the beginning of the spectrograph. The particles will then converge towards the detector through the rest of the magnet gap, and there is very little chance for scattering off the large surfaces of the pole pieces or from the edges of diaphragms placed between the pole pieces.

A single-gap spectrograph is usually designed so that it can be rotated about a vertical axis through the target. For mechanical reasons, it is difficult with such an instrument to reach the back angles (close to $\theta = 180$ deg). The multiple-gap spectrograph described below, however, covers angles up to 172.5 deg, and for some reactions these back angles are quite important.

It is generally desirable that the spectrograph admit in one exposure the full momentum range of the particles to be studied from one bombardment. This may often include more than one type of particle. Not only is the large range important for speed in data collection, but the simultaneous collection of the whole spectrum guarantees that conditions are exactly identical for each energy group. Then changes in target composition, incident energy and so forth will not cause one side of the spectrum to be recorded under different conditions than the other.

In a nuclear reaction, as pictured in figure 3 for instance, the recoil kinetic energy imparted to the residual nucleus depends upon the reaction angle θ. Therefore when the residual nucleus is left in a given energy state, the energy of the emitted particle depends slightly upon θ. Since the spectrograph accepts particles emitted with reaction angles varying over a range (determined by the entrance aperture), a broadening of the peaks in the particle spectrum results. This has been called "kinematic broadening" or "Doppler broadening." Since there is a correlation between the particle energy and the angle through which it enters the spectrograph, it is relatively easy to correct for Doppler broadening. In particular, if the median plane of the spectrograph coincides with the reaction plane, the Doppler effect changes the coefficient a_{10} in equation 9 and can be corrected by displacing the detector in or out along the central ray.

Let me now describe some spectrographs that have been built and tested and, in general, have lived up to expectations. The most important properties of these instruments are listed in the table. Most of these spectrographs exist in several versions and sizes. In particular, the MIT broad-range spectrograph has been adopted in a number of laboratories throughout the world. The newest addition to the list, the split-pole spectrograph, has been built or is being built for about a dozen laboratories.

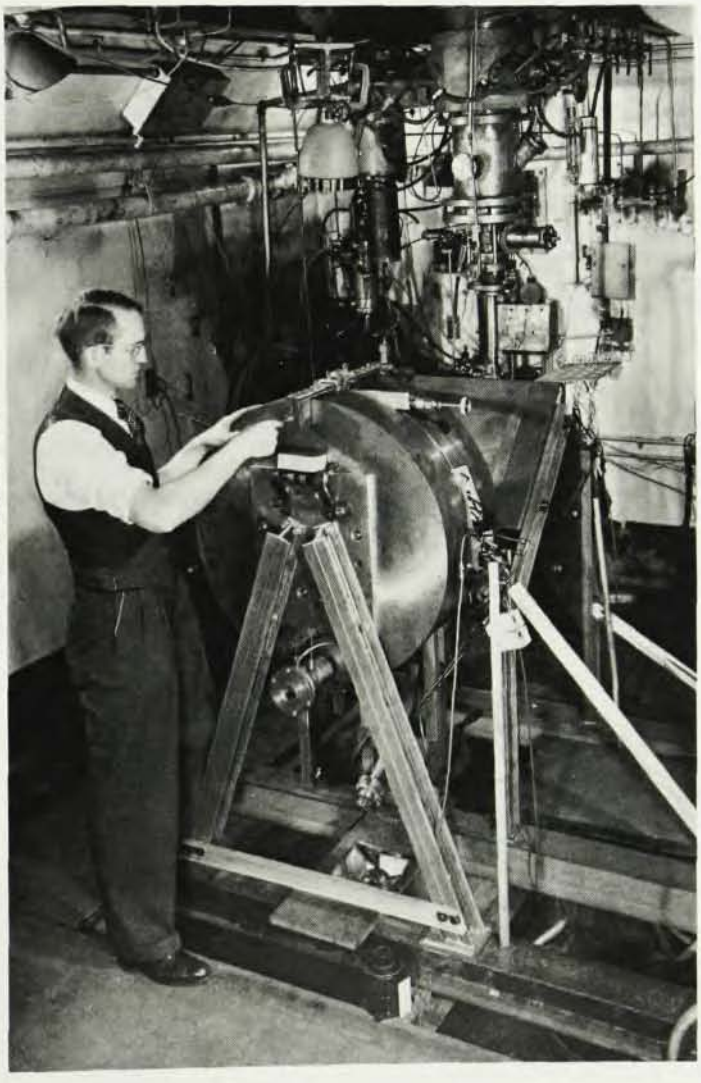

ANNULAR magnet at MIT was the first magnetic spectrograph used (1948) to detect charged particles emitted from nuclear reactions. —FIG. 4

The MIT annular magnet was the first magnetic spectrograph[2] to be used for the detection of charged particles emitted in nuclear reactions (1948). The Cal Tech instrument, described below, was, however, being tested simultaneously. The annular magnet is a homogeneous-field magnet utilizing 180-deg focusing. That is, in principle, it is a 180-deg sector, for which the object and image distances become zero. The target and detector (nuclear-track plate) were inside the field. The beam entered through a slot in the pole parallel to the field lines and was therefore not deflected. With this arrangement, the reaction angle was fixed at 90 deg. The annular magnet was used for a long series of nuclear-reaction studies in conjunction with the large MIT air-insulated 2-Me-V Van de Graaff accelerator (figure 4) and later with the 8-MeV MIT-ONR generator. It was retired in 1954. The median plane optics of the annular magnet are shown in figure 5a.

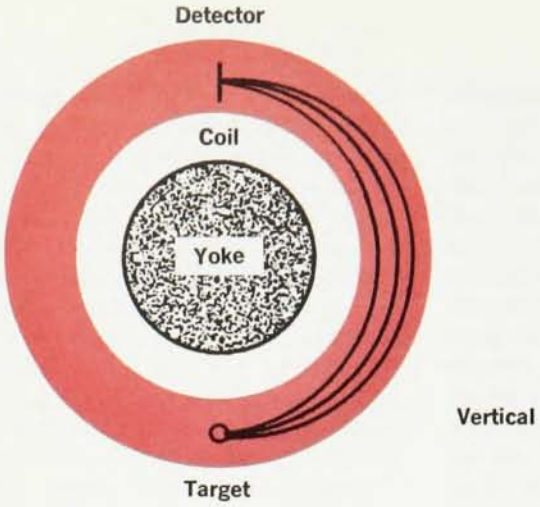

MIT Annular

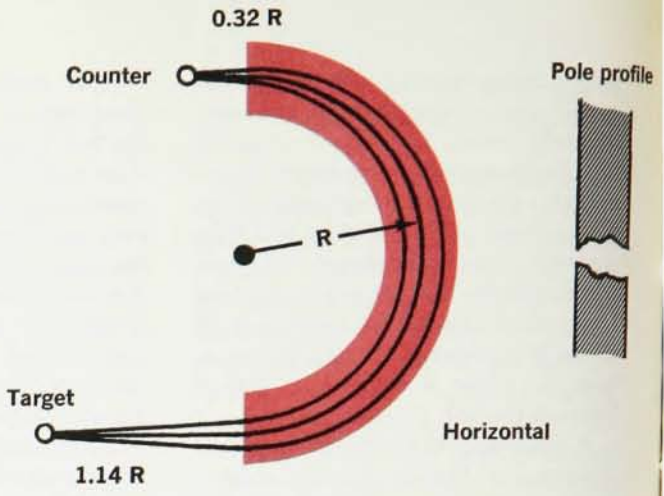

Cal Tech n = ½

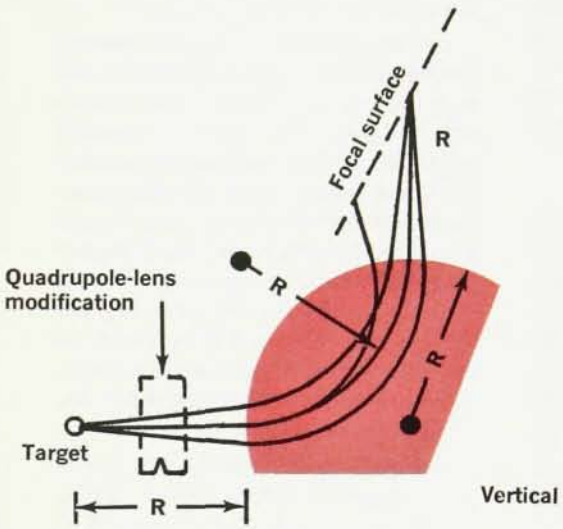

MIT Broad-Range

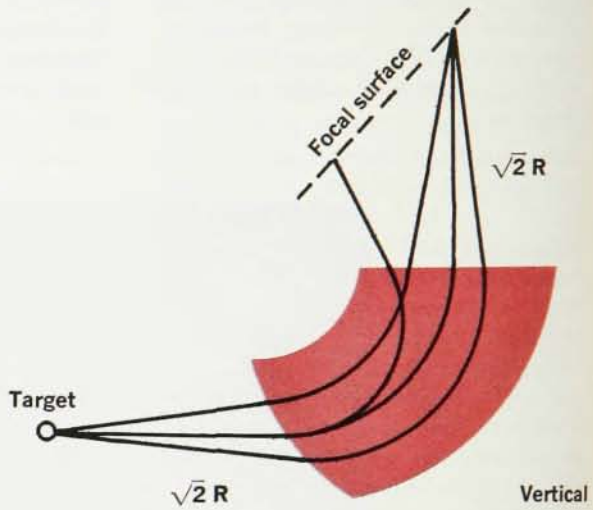

A.E.S. Green

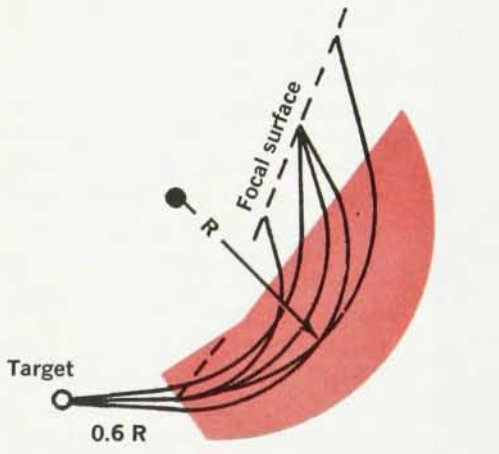

B. Elbek

MEDIAN-PLANE OPTICS of various magnetic spectrographs.—FIG. 5

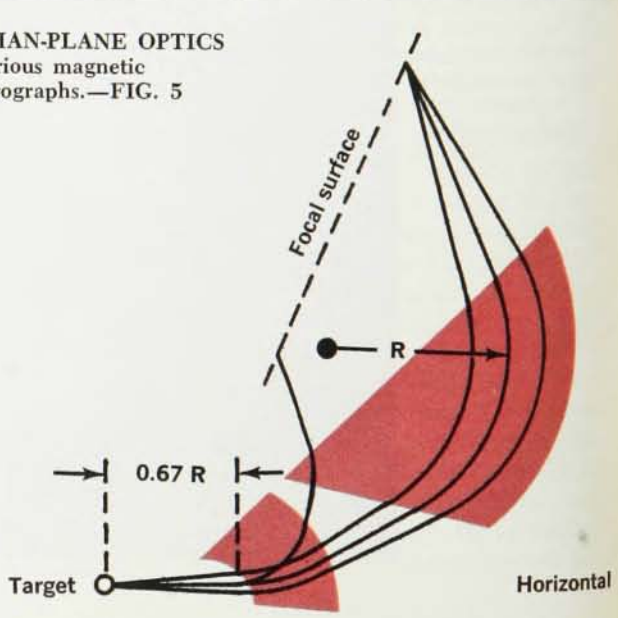

Split-Pole

The nuclear-emulsion technique was developed and used for direct studies of cosmic-ray and other nuclear events at about the time the MIT annular magnet was constructed. The MIT group adopted nuclear-track plates as the detector for the spectrograph, and it is remarkable that this technique after 20 years is virtually unchanged and is still the principal method of detection in spectrograph work at these energies. Since the particles were already momentum analyzed and oriented by the magnet, the plates were merely used as position indicators. They were scanned in half-millimeter strips, and different kinds of particles could be distinguished by their track lengths. The range covered by the nuclear-track plate in the annular magnet was quite small $p_{max}/p_{min} \approx 1.05$, limited by the narrow annular region of usable field. The corresponding length of a plate was of the order of 4 cm, and scanning over 0.5-mm strips therefore yielded about 80 data points. The resolution of the instrument was limited by the spot size of the beam on the target; a maximum of $p/\Delta p = 1600$ was recorded.

The 180-deg Cal Tech instrument. The inhomogeneous betatron-type field mentioned earlier was first used in a beta spectrograph by Nils Svartholm and Kai Siegbahn and is, incidentally, also used in modern ironless beta spectrographs of outstanding precision. In this type of instrument both the source and the detector are inside the magnetic field and focus is achieved after a deflection of 254 deg. The same type of field was first used for a nuclear-particle spectrograph at Cal Tech.[3] In the Cal Tech instrument, the deflecting angle is 180 deg, and the source and image are both outside the field. The detector was originally a slit-and-counter arrangement, but nuclear-track plates have also been used. Similar instruments have been built at a number of institutes, both for analyzing charged particles emitted in nuclear reactions and for studies of electron scattering. Figure 5b shows the optical layout of the original Caltech instrument.

MIT broad-range spectrograph. Figure 5c illustrates the focusing principles of the MIT broad-range spectrograph magnet.[4] It is actually a sector magnet but with curved entrance and exit surfaces as suggested by Kenneth Bainbridge.[5] The curvature produces second-order correction ($a_{20} = 0$, equation 9) for particles that are deflected by 90 deg, but the magnet has substantial second-order aberration for particles of higher and lower momenta. The spectrograph is used with three 2 × 10-inch nuclear-track plates as detectors. The total momentum range used is $p_{max}/p_{min} \approx 1.5$. Half-millimeter strips are scanned across the nuclear-track plates, and therefore about 1500 data points are obtained per exposure.

The solid angle of acceptance for the MIT broad-range spectrograph, as normally operated, is 0.4 msr, which is quite small if the instrument is to be used with a single counter as detector, for instance, in coincidence work. A modification of the broad-range spectrograph has a quadrupole lens between the target and the spectrograph entrance.[6] When the lens is turned off, the spectrograph works as a conventional broad-range instrument. When the lens is turned on, the angle of acceptance in the transverse direction is increased by a factor of approximately 10, while the angle of acceptance in the median plane decreases by a factor of 2. The net gain in solid angle is therefore approximately 5. The first instrument of this kind was built for the Chalk River Laboratories and has a total solid angle of 8 msr. When used in conjunction with the quadrupole lens, the median plane of the instrument is horizontal; that is, it coincides with the reaction plane. Doppler correction can then be achieved, as described above, by moving the detector in towards the magnet.

The MIT multiple-gap spectrograph. Imagine a doughnut with a cross section like the magnet of figure 5c. Slice up two quadrants of it in 7.5-deg sectors to produce air gaps. Drill a hole for the beam and put a target in the center of the doughnut. This is the idea of the multiple-gap spectrograph.[7] The instrument is 25 broad-range spectrographs with a common magnetic circuit operating all at once. The reaction angles covered are 0 to 172.5 deg in 7.5-deg steps. There are two 90-deg gaps, and the zero-degree gap is not normally usable. Counting 1500 data points at 23 different angles, one then gets a total of 34 500 data points per exposure. Figure 6 is a photo of the MIT multiple-gap spectrograph. The complete instrument is in a large vacuum tank. In the photograph, the top section of the tank has been removed.

Alex E. S. Green's spectrograph[8] built at Florida State University has

MIT MULTIPLE-GAP spectrograph set in large vacuum tank. —FIG. 6

an entrance angle (α, figure 2) of 35 deg, a deflection angle of 90 deg for a central momentum, and an exit angle of approximately zero degrees (figure 5d). The entrance boundary is curved to produce second-order correction. For a central momentum, the transverse focus is at infinity. A point source, therefore, produces a line focus on the detector. Since the spectrograph is mounted with the median plane vertical, that is, perpendicular to the reaction plane, the Doppler effect results in a twisting of the image line rather than a broadening of the image. The momentum range of Green's spectrograph is $p_{max}/p_{min} = 2.2$, and the maximum solid angle is about 10 msr.

Elbek's spectrograph. Figure 5e shows the layout of a broad-range spectrograph devised by Bent Elbek[9] and built for the Danish tandem accelerator facility. The entrance angle α is 35 deg, but since the object distance is shorter than in Green's spectrograph, a real transverse image is not produced. However, the focusing effect of the entrance fringing field produces some enhancement of the collecting power of the spectrograph.

The most remarkable property of Elbek's spectrograph is the almost complete absence of second-order aberration over the full momentum range, $p_{max}/p_{min} = 2.5$. Another important feature is that the magnification in the median plane is approximately $^1/_2$. This is important for attaining high resolving power (equation 8), and also for high accuracy because of the difficulty, in nuclear-reaction work, of maintaining an exact position of the beam spot on the target. The smaller the magnification, the less is the resultant motion of the image point. Two large spectrographs of Elbek's type have been built in this country, one for the Los Alamos Scientific Laboratory and one for Oak Ridge National Laboratory.

The split-pole spectrograph (figure 5f) has the same advantages as Elbek's spectrograph, and it goes a step further in that it has point-to-point focusing or approximately that for the full momentum range. This has been accomplished by splitting the pole pieces in two pairs and by shaping the split between them in such a fashion that high-momentum particles, qualitatively speaking, experience strong focusing forces twice in the fringing fields and low-momentum particles only once. In the split-pole spectrograph, as well as in Elbek's spectrograph, Doppler correction is achieved by detector displacement. The split-pole has the highest D/M ratio of spectrographs in the table mainly because the median-plane magnification is small: $M \approx 0.3$.

Split-pole spectrographs have been in operation for some time at the University of Pittsburgh and at the University of Rochester, both in conjunction with Tandem Van de Graaff accelerators. Figure 7 shows a small part of a spectrum obtained on the Rochester split pole with a position-sensitive solid-state detector as recorder. The process is $Tb^{159}(d,d')Tb^{159}$ at a reaction angle of $\theta = 40$ deg and with an incident energy of 18 MeV. The spectrum shows the elastic peak and two inelastic peaks corresponding to excited states in Tb^{159} at 58 and 137 keV. Two small peaks resulting from contaminants are also seen. Figure 8 is a photograph of the Rochester spectrograph.

Detectors for spectrographs

Most of the instruments mentioned above have been designed primarily for use with nuclear-track plates as recorders. These simple devices are unbeatable for reliability and simplicity and do not in any way impair the inherent resolving power of the rest of the instrumentation. The plates obviously can not be used for coincidence work or be a part of an on-line system, and data extraction is rather slow and tedious. Scanning 0.5 mm strips approximately 1 cm long, a plate scanner covers about 2 to 3 cm^2 of plate per hour, less if the intensity is high.

Many attempts have been made to develop detectors that can replace the nuclear-track plates. Position-sensitive solid-state detectors are being used with good results, but they are very limited in range. Sonic spark chambers are being tested. In one type the particle goes through a flat proportional counter and then through a flat spark chamber. A signal from the proportional counter triggers the high voltage on the spark chamber, a

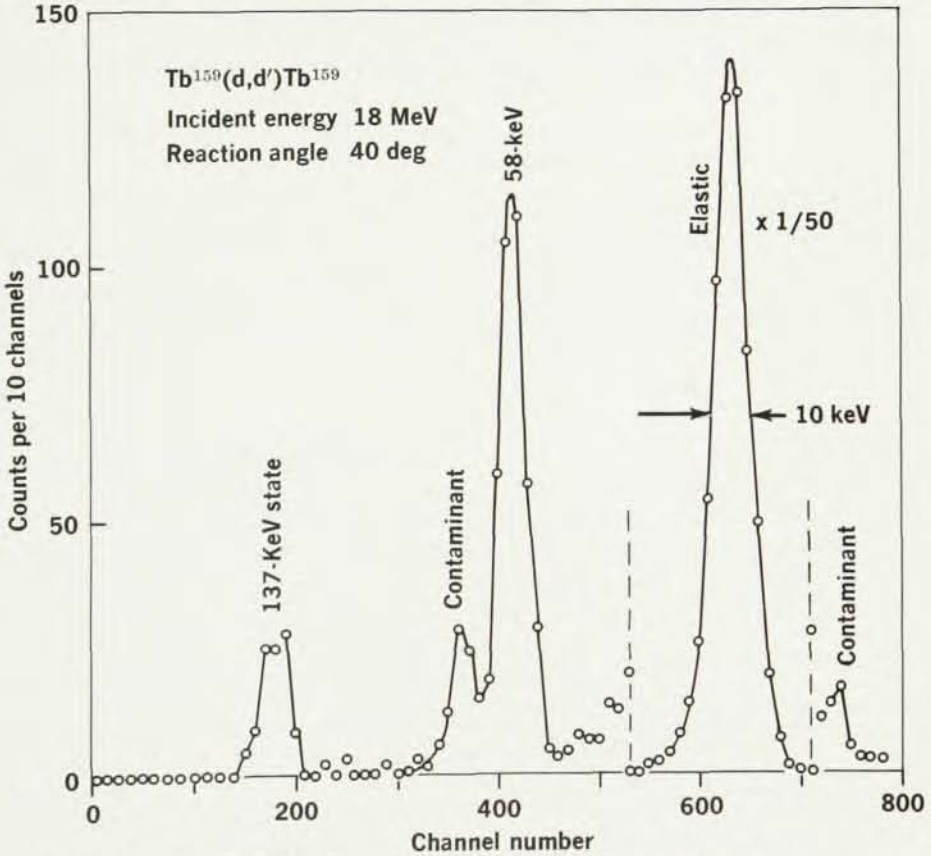

PART OF A SPECTRUM taken with a split-pole spectrograph from the $Tb^{159}(d,d')Tb^{159}$ reaction with 10-keV resolution. —FIG. 7

TEAR OUT THIS PAGE

check the TRW Image Converter Camera application papers you're interested in, fill in the form below, and we'll get the papers off to you within a day or two.

- ☐ USE OF TELEVISION WITH THE TRW IMAGE CONVERTER CAMERA FOR REMOTE READOUT AND ENHANCED SENSITIVITY, by T. H. Bulpitt
- ☐ LASER MODE STUDIES, by W. W. Simmons and R. S. Witte
- ☐ OBSERVATIONS OF RESISTIVE INSTABILITIES IN A THETA PINCH, by H. A. Bodin
- ☐ PLASMOID ROTATION IN A THETA PINCH, by G. L. Clark and R. F. Wuerker
- ☐ HOLE-BURNING MODEL OF OSCILLATION OF RUBY LASER, by A. J. DeMaria and R. Gagosz
- ☐ HIGH-SPEED PHOTOGRAPHIC STUDY OF THE STRUCTURE OF RUBY LASER EMISSIONS, by G. L. Clark, S. L. Ridgway, R. F. Wuerker and C. M. York, Jr.
- ☐ EXPLODING WIRE-DRIVEN SHOCK WAVE, by G. L. Clark and R. F. Wuerker
- ☐ A RADIATIVE DETONATION MODEL FOR THE DEVELOPMENT OF A LASER-INDUCED SPARK IN AIR, by S. A. Ramsden and P. Savic
- ☐ HIGH-SPEED PHOTOGRAPHIC INSTRUMENTATION OF BACK-ILLUMINATED EVENTS, by TRW Instruments Staff
- ☐ TIME-RESOLVED SPECTRA WITH THE 1D IMAGE CONVERTER CAMERA AND f/6.3 PLANE GRATING SPECTROGRAPH, by TRW Instruments Staff
- ☐ PRECISION RANGE-GATED IMAGING TECHNIQUES, by Don B. Neumann
- ☐ HIGH-SPEED PHOTOGRAPHIC INVESTIGATION OF GUN-LAUNCHED PROJECTILES, by John O. Clayton and Isaac Shanfield
- ☐ SUBNANOSECOND LIGHT PULSE MEASUREMENT WITH THE TRW IMAGE CONVERTER CAMERA, by TRW Instruments Staff

and these characteristic sheets

- ☐ CHARACTERISTICS OF THE TRW IMAGE CONVERTER CAMERAS
- ☐ CHARACTERISTICS OF THE TRW HIGH APERTURE TRANSMISSION SPECTROGRAPH
- ☐ CHARACTERISTICS OF THE TRW SUBMICROSECOND 5 FRAME PLUG-IN UNIT

TRW INSTRUMENTS
Dept. PT-767
139 Illinois St., El Segundo, Calif. 90245
(213) 679-9101 Extension 66884

NAME _____

COMPANY OR UNIVERSITY _____ TITLE _____

ADDRESS _____

CITY _____ STATE _____ ZIP _____

spark develops along the path of ions left by the particle, and the position of the spark is detected by measuring the time the sound of the spark takes to travel to a transducer at one end of the detector. Finally, wire spark chambers, which have been very successfully used in high-energy work (See Winslow Baker's article p. 41, this issue), are now being tested as detectors for low-energy spectrographs. The chamber has a flat high-voltage electrode facing an array of closely spaced wires. Each wire is connected to a magnetic-core memory, and the current from a spark sets up the memory. After the event the system reads out which core has been set up, and hence the position of the spark can be determined. The high voltage is triggered by a scintillation counter behind the spark chamber. The signal from the scintillation counter can be used for particle identification.

Cost of low-energy spectrographs

There are now a number of competent manufacturers of magnetic spectrographs for low-energy work. Any of the instruments discussed above can be made to order, complete with target chamber, power supply, fluxmeter, vacuum system, detector housing, rotating mount, etc. For a given maximum orbit radius R and maximum induction B, the cost of the magnet itself may differ somewhat from one type to another. The cost of the auxiliary equipment, however, varies very little, and this, of course, reduces the percentage difference in the total cost. As a first guess, the following formulas can be used for the total cost in the United States of a spectrograph with a maximum radius ranging from $R = 0.5$ to $R = 1.2$ meters and maximum induction $B \approx 15$ kilogauss:

$$\text{single-gap} \approx (50R + 120R^2)\ (\$10^3)$$
$$\text{multiple-gap} \approx (150R + 300R^2)(\$10^3)$$

Most manufacturers use special low-carbon steel in the pole pieces and less expensive steel, for example, C1010, in the yokes. The above costs are based on the assumption that this custom is followed.

Spectrograph trends

The trend in modern spectrograph design is definitely towards a larger number of adjustable parameters. A single deflecting magnet with straight boundaries, has three adjustable parameters: The entrance and exit angles α and β (also called shim angles), and the deflecting angle ϕ. The effect of a change in the entrance or exit angle is exactly the same as if a quadrupole lens were placed at the entrance or exit. The three parameters of the deflecting magnet are therefore really equivalent to two quadrupole magnets and a deflector with normal entrance and exit (dipole). If both of the pole boundaries at entrance and exit of the deflecting magnet are made curved and the radii of curvature regarded as adjustable parameters (at least they are adjustable in the design stage), the deflecting magnet becomes a five-parameter magnet. The curvatures are exactly equivalent to hexapole lenses (also called sextupoles). They have three north poles alternated with three south poles around the axis. For the split-pole spectrograph, mentioned above, eight parameters were varied in the design, and in a newer low-intensity, high-resolution version of the same instrument, ten parameters are varied. The two new parameters are third-order curvatures on two of the pole boundaries (octupoles).

A second trend is certainly one toward larger instruments, demanded of course mainly by the higher energies attained on modern accelerators. Thirdly, concentrated efforts are being made to integrate, or match, the spectrographs with the beam-handling systems of these modern accelerators.

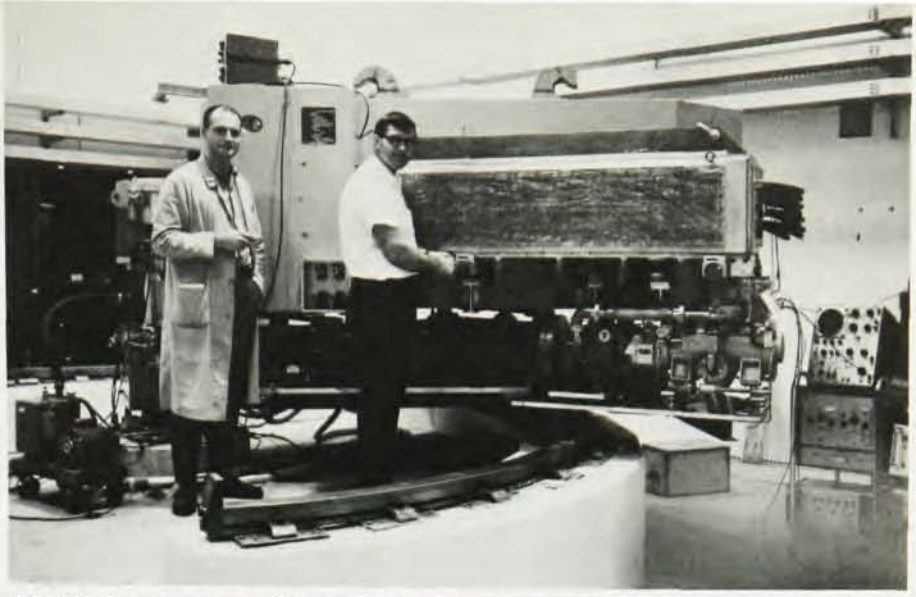

SPLIT-POLE spectrograph installed at the University of Rochester for use in conjunction with their Emperor Tandem Van de Graaff. —FIG. 8

Finally, more attention is being, and will continue to be, directed toward background suppression. In nuclear-structure physics some very interesting experiments can be performed if reaction products can be studied at $\theta = 0$. This is a formidable task even if the magnetic rigidities of the particles are well separated, since the beam intensity may be 10^{13} particles per second compared to maybe 10^2–10^3 particles per second of reaction products. We are working on new type devices for the purposes described here.

References

1. J. Ballam, PHYSICS TODAY, **20**, no. 4, 43 (1967).
2. W. W. Buechner, R. J. Van de Graaff, E. N. Strait, C. G. Stergiopoulos, A. Sperduto, Phys. Rev. **74**, 1226A (1948); Phys. Rev. **74**, 1570 (1948).
3. C. W. Snyder, S. Rubin, W. A. Fowler, C. C. Lauritsen, Rev. Sci. Instr. **21**, 852 (1950).
4. W. W. Buechner, C. P. Browne, H. A. Enge, M. Mazari, C. D. Buntschuh, Phys. Rev. **95**, 609A (1954); C. P. Browne, W. W. Buechner, Rev. Sci. Instr. **27**, 899 (1956).
5. K. T. Bainbridge, in *Experimental Nuclear Physics*, Part V (E. Segré, ed.) Wiley, New York (1952).
6. H. A. Enge, Rev. Sci. Instr. **29**, 885 (1958).
7. H. A. Enge, W. W. Buechner, Rev. Sci. Instr. **34**, 155 (1963).
8. A. E. S. Green, R. J. Berkley, C. E. Watson, C. F. Moore, Rev. Sci. Instr. **37**, 415 (1966).
9. J. Borggren, B. Elbek, L. P. Nielsen, Nucl. Instr. and Meth. **24**, 1 (1963).
10. H. A. Enge, Nucl. Instr. and Meth, **28**, 119 (1964); J. Spencer, H. A. Enge, Nucl. Instr. and Meth. **49**, 181 (1967). □